

Optimization of TiO₂ nanotubes synthesis on cylindrical surfaces for bio-implants

Gabriela Strnad^{1,*}, Laszlo Jakab-Farkas², Paul Chetan¹ and Cecilia Petrovan³

¹ “Petru Maior” University of Tirgu Mures, Faculty of Engineering, Department of Industrial Engineering and Management, Nicolae Iorga 1, Tirgu Mures, Romania

² Sapientia University of Cluj Napoca, Faculty of Technical and Human Sciences, Sighisoarei 1C, Tirgu Mures, Romania

³ University of Medicine and Pharmacy of Tirgu Mures, Faculty of Dental Medicine, Oral and Maxillofacial Surgery Department, Gh. Marinescu 38, Tirgu Mures, Romania

Abstract. Titanium based modified surfaces with TiO₂ self-organized nanotubular layers for biomedical applications were synthesized on cylindrical surfaces by electrochemical anodization in phosphate/fluoride electrolytes. Cylindrical samples of ϕ 3.8 x 20 mm, made of Ti6Al4V alloy, with different initial surface preparation (machined, grinded, polished) were subjected to anodization and process parameters were optimized to assure the development of uniform titania nanotubular layers with nanotubes' diameter of 25-100 nm. Optimal process parameters in our custom-built anodization cell are: electrolyte composition 1M H₃PO₄ + 0.4 wt% HF, anodization potential U = 24 V, potential ramp U_r = 0.08 V/s, distance anode-cathode d = 15 mm, current density in potentiostatic stage J = 35-50 A/m², and anodization duration t = 30-35 min.

1 Introduction

Clinical success of titanium-based biomedical implants used in dental and orthopedic applications relies on their biocompatibility, mechanical strength, and corrosion resistance. Surface related factors, such are roughness, wettability, and morphology, influence the osseointegration of titanium-based implants. The modification of surface at nanoscale level, to more closely resemble the surface topography of living tissue in order to get desirable cellular and tissue responses, is currently under an intense research focus. The covering of pure Ti and its alloys surfaces with layers of nanotubular TiO₂ (titania nanotubes – TNTs) with internal diameters of 15-100 nm is a recent approach that brings significant advantages in terms of osteogenesis at bone-implant interface [1-6].

By using electrochemical anodization (EA) method the surface modification at nanoscale level can be controlled. By changing EA process parameters: electrolyte composition, anodization potential, anodization time, different nano topographies can be achieved [7-12]. Phosphate-fluoride solutions used as electrolytes proved to be very effective on TiO₂ nanoporous/nanotubular self-organized structures synthesis. The presence of fluoride ions is the key factor that supports the complex mechanism and the delicate

*Corresponding author: gabriela.strnad@ing.upm.ro

balance between oxide formation and its dissolution that exists during the TiO₂ nanotubes growth. The anodization potential is of major importance having an essential influence on TNTs inner diameters. The anodization time controls the TNTs length.

There are many studies reporting TiO₂ nanotubes synthesis on extra polished planar surfaces of pure titanium. But the formation of TNTs on non-planar surfaces suffers from lack of investigation, on literature being little reports on this [13-14]. Also, the formation of self-ordered nanotubes on multi-phase titanium alloys is a more demanding process due to the preferential dissolution and different reactions rates of some phases of the alloy. TNTs synthesis on micro rough surfaces is another challenge that isn't properly addressed until now. In this context our recent work led to the optimization of EA process allowing the development, in a reproducible manner, of uniform, self-organized TiO₂ layers on the flat, polished or micro rough (turned, milled, sand blasted, sand blasted and acid etched) surfaces of pure titanium and dual phase ($\alpha+\beta$) Ti6Al4V alloy, in phosphate/fluoride-based electrolytes [15].

Present paper aims to optimize electrochemical anodization process for development of nanotubular TiO₂ layers on cylindrical surfaces of Ti6Al4V alloy, with different initial surface preparation: polished, grinded, and machined.

2 Methodology

Cylindrical samples of Ti6Al4V titanium alloy, with diameter of 3.8 mm and length of 20 mm were used in present set of experiments. Specimens were subjected to different initial manufacturing process: by CNC turning (resulting in a surface roughness R_a of $\sim 1 \mu\text{m}$), turning followed by grinding (surface roughness $R_a = 0.1\text{-}0.5 \mu\text{m}$), and turning, grinding and polishing (surface roughness $R_a = 0.01\text{-}0.1 \mu\text{m}$).

Turning was performed on Cincom K16 (Citizen) CNC turning machine. Wet grinding with 320-grit and 1200-grit papers was done for 5 minutes. Polishing was performed using 6 μm diamond suspension. Surftest SJ-310 (Mitutoyo) roughness tester was used for roughness measurements.

Prior to the electrochemical anodization process specimens were cleaned in several steps: ultrasonic bath with deionized water, ethyl alcohol, after then were dried in BOV-T25F (Biobase) drying unit.

The electrochemical anodization process was performed in a custom built electrochemical cell where the process parameters were controlled by an originally designed software - Nanosource 2 - which allows also the registration and visualization of process data. In the anodization cell the sample is connected to the anode, while the pure copper CuE cathode can be in various geometrical shapes: disc, annular with slits, flat foil. The distance anode-cathode was 15 mm for all experiments. Phosphate/fluoride-based electrolyte containing 1M H₃PO₄ and an addition of 0.4 wt% HF or 0.5 wt% HF was used as electrolyte in anodization experiments. Electrolyte was prepared from reagent grade chemicals (Chemical Company) and deionized water. Experiments were carried out at room temperature. Several experiments were conducted with anodization potentials of 20 V and 24 V, applied with a potential ramp of 0.1 V/s or 0.08 V/s. After the end potential was reached, we applied a potentiostatic stage by holding constant the end potential for an anodization time of 30 min. After anodization, the samples were rinsed with deionized water, cleaned in ethanol and dried.

The surface morphology was evaluated using scanning electron microscopy (SEM), performed in a JSM 5200 (JEOL) scanning electron microscope, operated at 25 kV. The dimensions of nanostructures developed on modified surfaces were measured on SEM micrographs using an open source graphical image processing software (Gimp).

3 Results and discussion

Experiments for development of nanostructured oxide layers on cylindrical surfaces were performed, initially, by using process parameters that provided the best results on flat surfaces in our anodization setup. Our results show that in the same conditions regarding initial surface preparation, electrolyte composition, anodization potential, potential ramp, and anodization duration the diameters of nanotubes developed on cylindrical surfaces are smaller than those developed on flat surfaces.

The results of SEM analysis for samples with initial microrough surface ($R_a = 1 \mu\text{m}$) anodized in $1\text{M H}_3\text{PO}_4 + 0.5 \text{ wt\% HF}$, anodization potential $U = 20 \text{ V}$, potential ramp $U_r = 0.1 \text{ V/s}$, anodization duration $t = 30 \text{ min}$, show the development of nanotubes/nanopores with internal diameter $D = 15\text{--}50 \text{ nm}$ (mainly 40 nm) on cylindrical surfaces (Figure 1a), and of nanotubes having $D = 25\text{--}90 \text{ nm}$ (mainly 70 nm) on flat surfaces (Figure 1b). Electric parameters monitoring during the EA allowed us to compare the current evolution in the process of nanostructured oxide layers' synthesis on cylindrical and flat surfaces, to ascertain the similarity of evolution, and to report a value of $30\text{--}40 \text{ A/m}^2$ for current density in the stage where the nanotubes are developing (Figure 1d).

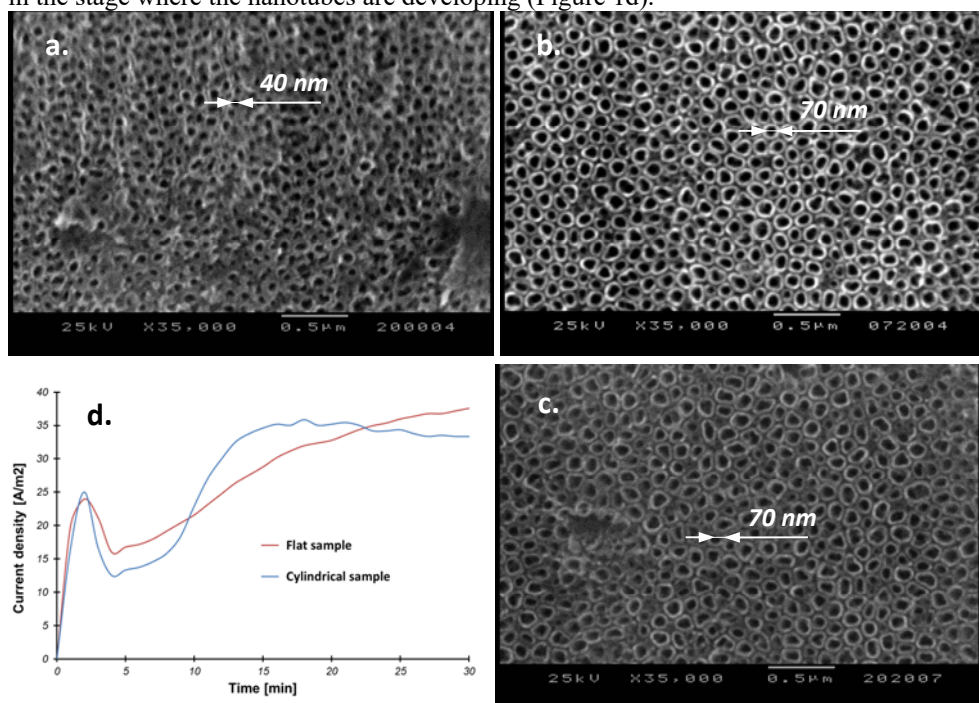


Fig. 1. SEM micrographs of nanostructured oxide layers developed on Ti6Al4V microrough surface: a – cylindrical surface ($1\text{M H}_3\text{PO}_4 + 0.5 \text{ wt\% HF}$, $U=20 \text{ V}$, $U_r = 0.1 \text{ V/s}$); b – flat surface ($1\text{M H}_3\text{PO}_4 + 0.5 \text{ wt\% HF}$, $U=20 \text{ V}$, $U_r = 0.1 \text{ V/s}$); c - cylindrical surface ($1\text{M H}_3\text{PO}_4 + 0.4 \text{ wt\% HF}$, $U=24 \text{ V}$, $U_r = 0.08 \text{ V/s}$); d - current density during anodization of samples a and b; Magnification: 35000X.

The same results showing the synthesis of nanotubes with smaller diameters on cylindrical surfaces compared with flat surfaces, in the same EA process conditions, were obtained by us on polished samples ($R_a = 0.05 \mu\text{m}$): $D = 25\text{--}100 \text{ nm}$ on cylindrical surfaces, compared with $D = 50\text{--}120 \text{ nm}$ on flat surfaces.

These results led us to the conclusion that we need to increase the anodization potential in order to develop nanotubes with internal diameters in $15\text{--}100 \text{ nm}$ range on cylindrical surfaces. Optimization experiments allowed us to find that in our anodization cell the best

process parameters of EA are: *electrolyte composition* 1M H_3PO_4 + 0.4 wt% HF, *anodization potential* $U = 24$ V, *potential ramp* $U_r = 0.08$ V/s, *anodization duration* $t = 30$ -35 min. By working in these conditions, the modified Ti6Al4V cylindrical surfaces are covered with continuous, uniform and well-developed nanotubular oxide layers. On microrough cylindrical surfaces the nanotubes' internal diameter is of $D = 25 - 90$ nm (mainly 70 nm), as Figure 1.c shows, being of the same dimensions as the nanotubes' developed on flat surfaces in optimized conditions for that kind of samples (Figure 1b).

Figure 2 presents the SEM micrographs, taken at low and high magnifications, of nanotubular layers developed in above mentioned optimized anodization conditions on cylindrical surfaces of Ti6Al4V alloy, showing the development of nanotubes of 25-100 nm in diameter on grinded (Figures 2a and 2c) and polished surfaces (Figures 2b and 2d).

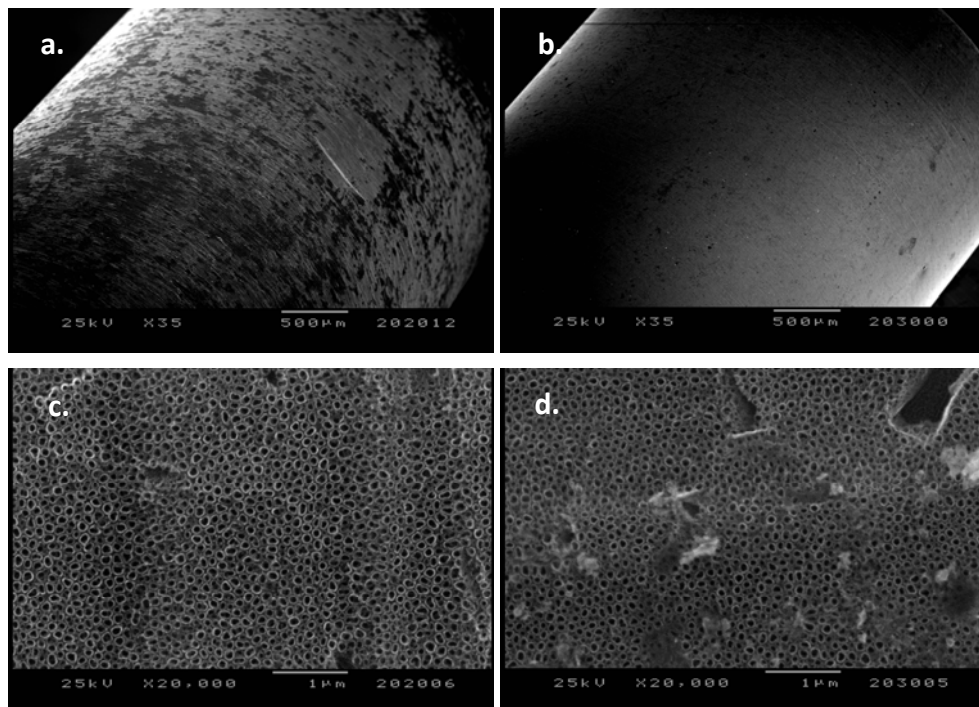


Fig. 2. SEM micrographs of nanotubular oxide layers developed on Ti6Al4V cylindrical surfaces by anodization in 1M H_3PO_4 + 0.4 wt% HF electrolyte, $U = 24$ V, $t = 35$ min; initial surface preparation: a, c – grinded surface, $R_a = 0.5$ μ m; b, d – polished surface, $R_a = 0.05$ μ m; Magnification: a, b - 35X; c, d - 20000X.

The anodization experiments conducted in optimized conditions were performed with several types of cathodes, regarding their geometrical shape. Disc, annular with slits and flat foil copper cathodes were used (Figure 3). The electrical parameters were monitored and registered in real time during the nanostructured layers development, by using our originally developed Nanosource 2 software.

The results show a robust anodization process, resulting in well-developed nanotubular layers on cylindrical surfaces by using all three types of cathodes (Figures 4a, b, and c). SEM micrographs analysis shows a better uniformity of the modified oxide nanostructured layer in the case of annular cathode with slits. This can be explained by the fact that in this case the cathode is all around the cylindrical sample, by this the electrical field lines are better closed, and the slits allow a proper circulation of electrolyte in anode-cathode space. The current density shows a similar evolution for all three types of cathodes, the current-

time characteristics present the steady state stage, where the current density is constant, $J = 35-50 \text{ A/m}^2$, and during which the nanotubular morphology is developing on the cylindrical samples surfaces (Figure 4d).

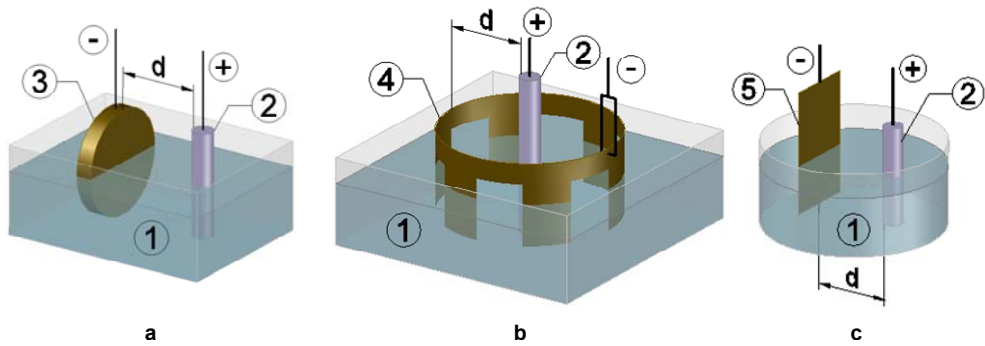


Fig. 3. Anodization bath setups for cylindrical samples using: a - disc cathode; b – annular cathode with slits; c - flat foil cathode; 1 - electrolyte; 2 – titanium alloy cylindrical sample; 3 – disc cathode; 4 - cylindrical foil with slits cathode; 5 – flat foil cathode.

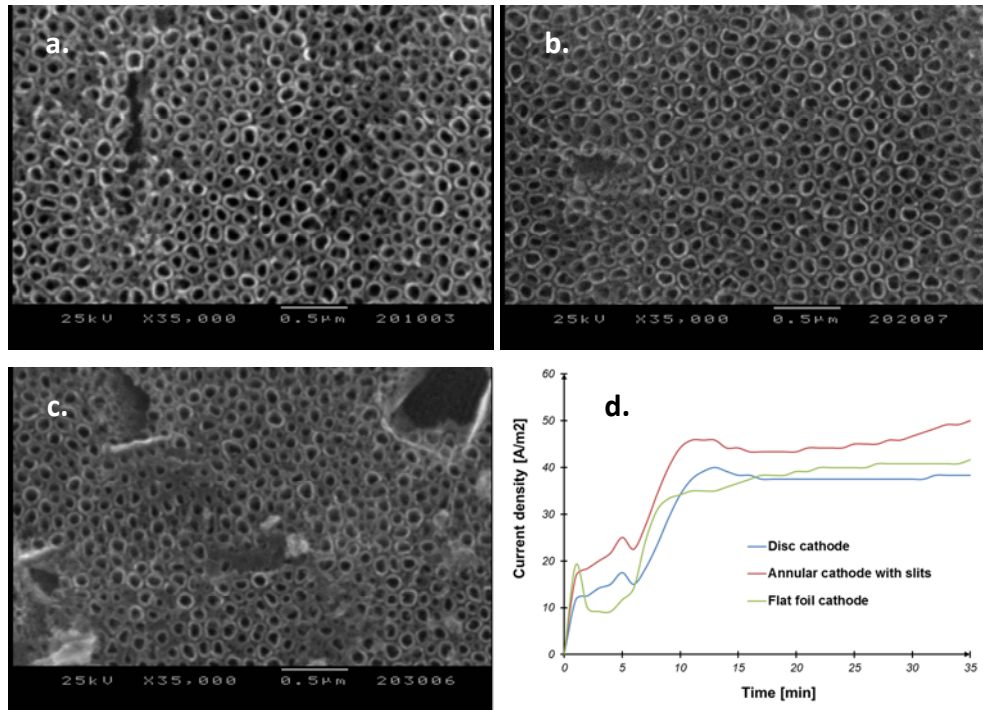


Fig. 4. SEM micrographs of nanotubular oxide layers developed on Ti6Al4V cylindrical surfaces by anodization in $1\text{M H}_3\text{PO}_4 + 0.4 \text{ wt\% HF}$ electrolyte, $U = 24 \text{ V}$, $t = 35 \text{ min}$, by using: a – disc cathode; b – annular cathode with slits; c- flat foil cathode; d – current density during anodization; Magnification: 35000X.

4 Conclusions

The synthesis of oxide layers with nanotubular morphology on cylindrical surfaces of two phase ($\alpha+\beta$) Ti6Al4V alloy by electrochemical anodization in phosphate/fluoride solutions

was optimized in order to ensure the development of nanotubes with internal diameters in 15-100 nm range, requested by medical applications for an enhanced osseointegration.

Our results show the development of well defined, self-arranged oxide nanotubes on the cylindrical surfaces by EA in 1M H₃PO₄ with an addition of 0.4 wt% HF electrolyte, at anodization potential of 24 V, applied with a potential ramp of 0.08 V/s, for an anodization duration of 30-35 min. In these conditions, the nanotubular morphology, with nanotubes having internal diameter of nanotubes in 25-100 nm range, is developing regardless the initial cylindrical surface preparation (turned, grinded, polished), and the cathode shape (disc, annular with slits, flat foil). The current density in anodization cell during the stage of nanotubes growth is in 35-50 A/m² range.

Our results present elements of novelty compared with the state of the art, by reporting the optimized process parameters for the synthesis, in a reproducible manner, of nanotubular self-organized oxide layers on cylindrical microrough surfaces ($R_a = 0.1-1 \mu\text{m}$), not only on polished surfaces. By these, significant advantages in terms of manufacturing process of advanced medical implants with nanostructured surfaces can be brought.

This work was supported by a grant of the Romanian National Authority for Scientific Research and Innovation, CNCS/CCCDI-UEFISCDI, project number PN-III-P2-2.1-PED-2016-0142, within PNCDI III.

References

1. K. Gulati, S. Maher, D. Findlay, D. Losic D., *Nanomedicine*, **11(14)** 1847–1864 (2016)
2. A. R. Ribeiro, S. Gemini-Piperni, S.A. Alves, *Metal Nanoparticle in Pharma*, doi.org/10.1007/978-3-319-63790-7_6, 101-121 (2017)
3. R. R. Baena, S. Rizzo, L. Manzo, S. M. Lupi, *Journal of Nanomaterials*, **2017** 6092895 (2017)
4. K. Gulati, I. Saso, *Expert Opinion on Drug Delivery*, **14(8)** 1009-1024 (2017)
5. M. Jäger, H. P. Jennissen, F. Dittrich, A. Fischer, *Materials*, **10(11)** 1302 (2017)
6. Y. Huang, X. Shen, H. Qiao, H. Yang, X. Zhang, Y. Liu, H. Yang, *International Journal of Nanomedicine*, **13** 633–640 (2018)
7. P. Roy, S. Berger, P. Schmuki, *Angewandte Chemie Internat.*, **50** 2904 – 2939 (2011)
8. M. Kulkarni, A. Mazare, P. Schmuki, A. Iglic, *Adv. Mat. Letters*, **7(1)** 23-28 (2016)
9. U. H. Shah, K. M. Deen, H. Asgar, Z. Rahman, *Journal of Electroanalytical Chemistry*, **807** 228-234 (2017)
10. A. B. Stoian, M. Vardaki, D. Ionita, M. Enachescu, M. Prodana, O. Brancoveanu, I. Demetrescu, *Ceramics International*, **44** (6) 7026-7033 (2018)
11. M. Yu, H. Cui, F. Ai, L. Jiang, J. Kong, X. Zhu, *Electrochemistry Communications*, **86** 80–84 (2018)
12. H. Li, M. Ding, J. Jin, D. Sun, S. Zhang, C. Jia, L. Sun, *ChemElectroChem*, [doi: 10.1002/celec.201701231](https://doi.org/10.1002/celec.201701231) (2018)
13. K. Gulati, A. Santos, D. Findlay, D. Losic, *Journal of Physical Chemistry C*, **119** 16033–16045 (2015)
14. T. Monetta, A. Acquesta, A. Carangelo, F. Bellucci, *Metals*, **7** 167 (2017)
15. G. Strnad, R. Cazacu, P. Chetan, Z. German-Sallo, L. Jakab-Farkas, *MATEC Web of Conferences*, **137** 02011 (2017)